Impact of Simulated Irrigation with Treated Wastewater and Saline-Sodic Solutions on Soil Hydraulic Conductivity, Pores Distribution and Fractal Dimension

Fangze Shang, Shumei Ren, Tian Zou, Peiling Yang, Nuan Sun

Impact of Simulated Irrigation with Treated Wastewater and Saline-Sodic Solutions on Soil Hydraulic Conductivity, Pores Distribution and Fractal Dimension

Fangze Shang[1,a], Shumei Ren[1,b], Tian Zou[1,c], Peiling Yang[1,d], Nuan Sun[1,e]

[1]College of Water Resources and Civil Engineering, China Agricultural University, Beijing 100083, China

[a]shangfangze@126.com, [b]renshumei@126.com, [c]zoutian066@126.com, [d]yangpeiling@126.com, [e]aile007@yeah.net

Abstract. Irrigation with treated wastewater which has the characteristics of higher salt content, larger sodium adsorption ratio (SAR), and more organic matter and suspended particles can cause the deterioration of the soil environment. Ordinary water, treated wastewater, and saline-sodic solutions with SAR = 3, 10 and 20 $(mmol_c \cdot L^{-1})^{0.5}$, respectively, were used as five irrigation water types, and the changes of soil saturated hydraulic conductivity (K_s), soil pores distribution, and soil pores single fractal dimension (D_m) were studied after simulated irrigation for 1 and 2 years with simulated irrigation systems, which consisted of soil bins and simulated evaporation systems. The results showed that soil K_s in the following descending order: CK > SAR3 > WW > SAR10 > SAR20, and the adverse effects on soil K_s caused by suspended solid particles and dissolved organic matter might play a more significant role than sodium in treated wastewater. The 0-5 cm soils had a smaller single soil pore area but larger pores quantity after simulated irrigation, the distribution of soil pores which was irrigated with treated wastewater had a smaller change compared with saline-sodic solutions treatments, and it showed the soil pores structure binary image was an effective method to analysis soil pores distribution. Soil D_m increased after simulated irrigation, and the smallest was the soil simulated irrigation with treated wastewater for 1 year, because the plugging and filling of suspended particles and dissolved organic matter in treated wastewater made the soil pores well distributed, but the soil D_m did not increase with increasing of SAR levels in irrigation waters. The relative SAR levels irrigation to soils and soil K_s had a good linear correlation relationship, while the relationship between soil D_m and the relative SAR levels irrigation to soils was very complicated. The soil D_m which calculated from soil binary images could not well reflect the hydraulic conductivity of saturated soil. Irrigation with treated wastewater had a greater effect on soil K_s than soil D_m, comparing with saline-sodic solutions which had the similar SAR value. It was suggested that the future research should consider both the horizontal and vertical directions of soil D_m to well reflect the soil K_s.

Keywords: treated wastewater, sodium adsorption ratio (SAR), soil saturated hydraulic conductivity (K_s), soil pore distribution, soil pore single fractal dimension (D_m), simulated irrigation

1 Introduction

China is one of the world's 13 severe water shortage countries, and it is also a large agricultural country, thus the shortage of water resources and the huge consumption of water in agriculture becomes a contradiction. The use of treated wastewater for agricultural irrigation provided a way to solve this contradiction [1]. However, the use of treated wastewater can cause the deterioration of the soil environment, such as soil saturated hydraulic conductivity (K_s) decrease and soil pore structure change.

The treated wastewater had the characteristic of higher salt content, larger sodium adsorption ratio (SAR), and more organic matter and suspended particles. For soils irrigation with saline-sodic water, the swelling and dispersion of clay particles were two major mechanisms responsible for reduction in hydraulic conductivity, and the plugging of soil pores by dispersed clay particles was a major cause [2-5]. But for soils irrigation with treated wastewater, organic matter and suspended particles caused physical and biological plugging to soil pores, and had more complex effect to soil hydraulic conductivity [6-7]. Some studies showed that when salt concentration was smaller than flocculating value of soil clay particles, the main factors which affect soil K_s was the dispersion of soil clay particles, while salt concentration was larger than flocculating value of soil clay particles, the main factors affect soil K_s was the swelling of clay soil particles [8]. High SAR in irrigation water had different effects on different soils, and many studies showed it had a larger effect on loam soil than sandy soil [9-11], which meant that the swelling and dispersion of clay particles had positive correlation with salt content and SAR in soil solutions. However, Singh et al [12] showed that the increase of SAR did not necessarily cause the decrease of soil hydraulic conductivity, after irrigation with water of SAR = 20 and 40, the soil K_s reduced by 12% and 7%, respectively, and when irrigation water with high salinity and SAR, the hydraulic conductivity did not reduce significantly. Therefore, the relationship between the irrigation water with different SAR levels and soil K_s is still less known.

Irrigation with high SAR water may cause the change of soil pores, and fractal dimension is an important index that describes the soil pores. Mandelbort [13] first proposed fractal theory was a nonlinear science theory which description the system that very complicated but had the scale invariance, and laid the foundation for using fractal theory study soils. Tyler and Wheatcraft [14] first applied the fractal geometry method to study the soil physics, and showed that soil pore shape had fractal characteristics, thus could describe by the fractal dimension. Perrier et al [15] also showed that soil pores structure exist self-similar phenomena, and showed an obvious fractal characters. Many studies used fractal method to carry on various researches about soil pores [16-19]. Some studies used image analysis to study soil pores structure [20-21]. Single fractal dimension and multifractal dimension had their respective advantages and disadvantages, and the single fractal dimension could describe the soil pores on the whole [22-25]. However, the study on the impact of long-term irrigation with different SAR levels waters on soil K_s and the fractal dimension are less, and the relationship between irrigation water SAR, soil K_s and the fractal dimension are also less known.

To our knowledge, the relationship between irrigation water SAR, soil K_s and the fractal dimension are less studied, and the difference among ordinary water, treated

wastewater and saline–sodic water on soil physical property are also less known. Thus, our objectives were: (1) to compare the impact of simulated irrigation with treated wastewater and saline-sodic solutions with different SAR levels on soil K_s, soil pores distribution and soil fractal dimension; (2) to explore the relationship between irrigation water SAR levels, soil K_s and fractal dimension.

2 Experiments and Methods

2.1 Simulated Irrigation Systems

The experiment was conducted in the experiment hall in the college of water resources and civil engineering of China Agricultural University during September to December, 2011. Simulated irrigation systems consisted of soil bins and simulated evaporation systems. The soil bins were built by clay soil, and daub cement on four sides of the soil bins, a total of five soil bins were built, and each had a length of 1.2 m, width of 1.2 m and high of 1.5 m. Waterproof adhesive were daubed at inside and the bottom of the soil bins, and form 1 mm thick waterproof layer. The soil bins bottom slope was 5^0, from down to up laid permeable fabric and inverted filter at the bottom of soil bins, and the inverted filter was made by quartz sand. After laid permeable fabric and inverted filter, 40 cm thick sandy soil was filled, then 80 cm thick loam was filled. The sandy soils were taken from Daxing district of Beijing, and the loam were taken from Tongzhou district of Beijing. In order to ensure tightly compacted soil bins, the soils were first through the 2 mm screen and slightly wetted and carefully mixed before packing. The soil bins were subsequently packed layer by layer in increments of 2 cm according to the actual field soil bulk density. The initial physical and chemical properties of experiment soils were listed in table 1. Simulated evaporation systems were including the first support, electric fan, distribution box, the second support and 275 W infrared light bulbs that installed in the second support. The first support erected in the upper part of the soil bin, and electric fan hanging in the first support. The second support fixed in the first support, and located below of the electric fan, three infrared light bulbs fixed on the two second support, respectively, electric fan and infrared light bulbs connected with distribution box through the wire, respectively. Simulated irrigation systems schematic diagram were shown in Fig.1.

Table 1. Initial physical and chemical properties of experiment soils

Soil types	pH	EC	Bulk density	Sand	Silt	Clay	Organic C
		($dS \cdot m^{-1}$)	($g \cdot cm^{-3}$)	%			
Loam	8.3	0.27	1.4	54.04	36.85	9.11	0.42
Sandy soil	8.4	0.25	1.4	88.48	8.13	3.39	0.19

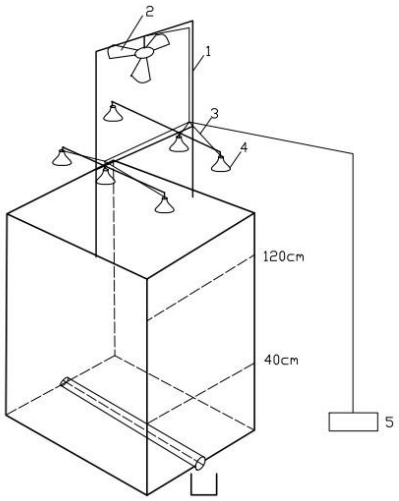

Fig. 1. Simulated irrigation systems schematic diagram (1: the first support; 2: the electric fan; 3: the second support; 4: the 275 w infrared light bulbs; 5: the distribution box).

2.2 Experimental Design

The treated wastewater was secondary precipitation water that taken from Qinghe sewage treatment plant of Beijing, ordinary water was tap water that taken from China Agricultural University. Using treated wastewater, ordinary water and deionized water to configurate five kinds of different SAR levels water. According to formula (1), quantitative NaCl and $CaCl_2$ (reagent grade) were added in deionized water to configurate saline-sodic solutions with SAR = 3, 10 and 20 $(mmol_c \cdot L^{-1})^{0.5}$, respectively. CK, WW, SAR3, SAR10 and SAR20 denoted ordinary water, treated wastewater, and saline-sodic solutions with SAR = 3, 10 and 20 $(mmol_c \cdot L^{-1})^{0.5}$, respectively. Relevant chemical characteristics of the five irrigation waters were presented in table 2. With reference to the winter wheat and summer corn irrigation quota in Beijing plain at normal rainfall, the winter wheat irrigation quota was 200 mm and 4 times irrigation, and the summer corn irrigation quota was 30 mm and 1 time irrigation in farmland, thus simulated irrigation water for each soil bin was 330 L for 1 year, irrigation water was 66 L at each soil bin at each time, and after 5 and 10 times irrigation, it means simulated irrigation for 1 and 2 years, respectively. After irrigation water for 66 L at each soil bin, electric fan opened 8 hours every day, and opened infrared light bulbs for 0.5 hour at the second, fourth, sixth and eighth day, respectively, 10 days later, irrigation with the same water again, a total of 10 times of cycle irrigation were conducted. After simulated irrigation for 1 and 2 years, sampling surface soil with cutting ring in order to measure soil K_s, three repetitions, and sampling 0-5 cm surface soil with density cutting ring to analysis soil fractal dimensions. CK-1, WW-1, SAR3-1, SAR10-1 and SAR20-1 denoted treatments that simulated irrigation for 1 year with ordinary water, treated wastewater, and saline-sodic solutions with SAR = 3, 10 and 20 $(mmol_c \cdot L^{-1})^{0.5}$, respectively, and CK-2, WW-2, SAR3-2, SAR10-2 and SAR20-2 denoted treatments that simulated irrigation for 2

year with ordinary water, treated wastewater, and salt solutions with SAR = 3, 10 and 20 $(mmol_c \cdot L^{-1})^{0.5}$, respectively.

$$SAR = \frac{Na^+}{\sqrt{Ca^{2+}}/2} \quad ---(1)$$

Table 2. Important chemical characteristics of the five water types used during simulated irrigation

Parameter	Irrigation water type				
	CK	WW	SAR3	SAR10	SAR20
pH	7.84	7.78	8.2	7.56	7.02
EC(dS m^{-1})	713.5	994	965	1043	1245
SAR($mmol_c$ L-1) $^{0.5}$	0.74	2.75	3	10	20
K^+(mg L^{-1})	8	8.91	0	0	0
Ca^{2+}(mg L^{-1})	52.36	96.59	286.93	83.25	25.27
Na^+(mg L^{-1})	14.5	106.13	282.55	497.25	558.35
Mg^{2+}(mg L^{-1})	18.91	40.66	0	0	0
Cl^-(mg L^{-1})	22.9	105	355	355	355
SO_4^{2-}(mg L^{-1})	75	104	0	0	0
HCO_3^-(mg L^{-1})	142	242	0	0	0
TSS[a](mg L^{-1})	3.5	21.3	0	0	0
BOD[b](mg O_2 L^{-1})	1.1	12.6	0	0	0
COD[c](mg O_2 L^{-1})	3.5	39.3	0	0	0

[a]TSS = total suspended solids, [b]*BOD = biological oxygen demand,* [c]*COD = chemical oxygen demand*

2.3 The Soil K_s Equation

In the measurement of soil K_s, the water flow was continuous, and the water temperature difference did not exceed 2 ^{0}C, and could be considered as isothermal, thus the experiment met the requirement of Darcian law´s laminar flow conditions, according to Darcian law formula (2), and combined with formula (3), we could launch soil K_s formula (4) in constant head:

$$q = K_s \frac{\Delta H}{L} \quad ---(2)$$

$$q = \frac{Q}{At} \quad ---(3)$$

$$K_s = \frac{QL}{A\Delta Ht} \quad ---(4)$$

Where q denoted water flux; K_s denoted soil saturated hydraulic conductivity; ΔH denoted total head of seepage path; L denoted straight line length of seepage path; Q denoted water volume; A denoted cross-sectional area of seepage and t denoted

seepage time.

2.4 Soil Thin Section Preparation

The soil thin section was made in the laboratory in the college of Materials Science and Technology of China University of Geosciences (Beijing). Preparation of soil thin sections was undertaken using standard procedures adapted from the method described by Murphy [26] and Guan et al [20]. Use density cutting ring to get 0-5 cm surface soil samples, collected samples were dried at 60 ^{0}C-80 ^{0}C in drying oven until water was completely evaporated, then cooled the samples to 40 ^{0}C, and took out the samples, then cut the intermediate section, and using coarse sandy paper (120$^{\#}$) to polish the soil until the soil thickness was 1 cm, then heated the samples to about 80 ^{0}C, afterwards, put epoxy resin and triethanolamine into the beaker at the ratio of 10:1, and heated them as curing agent, then put the samples into the beaker, made curing agent to penetrate completely into the samples. After that, put the samples on plate glass and fine grinding to 2 mm with emery. Put chromic oxide and oxalic acid into the beaker at the ratio of 3:1, added distilled water, and stir well as polishing liquid, using this polishing liquid to polish samples. At the end of the whole process, a soil thin section with side length of 7 mm, and thickness of 2 mm was obtained.

2.5 Digital Image Acquisition

The digital images were made in National Nonferrous Metal and Electronic Material Analysis Test Centre in General Research Institute for Nonferrous Metals of China. The digital images were obtained using a JEOL JSM-6510 scanning electronic microscope (SEM), and its resolution is 3.0 nm, magnification is 5X-300000X. A JS-1600 Small ion sputtering apparatus was also used in combined with scanning electronic microscope (SEM). The whole electronic micrograph was enlarged 55 times, then chosen areas were enlarged 200, 2000 and 5000 times. These three magnifications were compared, and the 200 times image was chosen as the image best representing soil structure [20]. The digital form of the picture was a grey level picture.

2.6 Image Segmentation

The goal of the soil image segmentation was extraction parameters from soil particles and pores, and quantitative analysis. The average grey value of edge point pixel method as image segmentation threshold value was used [27], and then used global threshold method to segmentation grey image, and then converted the segmentation grey image to binary image. In the soil binary images, the soil pores was black and solid was white. The threshold value of soil images was shown in table 3.

Table 3. The threshold value of soil images

Type	Threshold value	Type	Threshold value
CS[a]	61	SAR3-1	53
CK-1	66	SAR3-2	78
CK-2	66	SAR10-1	54
WW-1	59	SAR10-2	54
WW-2	81	SAR20-1	54
		SAR20-2	74

[a]CS = initial soil

2.7 Calculation methods of soil single fractal dimension

Soil single fractal dimension (D_m) quantitative described the complexity of the soil fractal, and the characteristic of soil fractal. Small island method was used to calculate soil D_m. Mandelbrot et al [28] pointed:

$$\alpha_D(\varepsilon) = \frac{\bar{L}^{\frac{1}{D}}(\varepsilon)}{\bar{A}^{\frac{1}{2}}(\varepsilon)} \quad ---(5)$$

$$logL(\varepsilon) = Dlog\alpha_D(\varepsilon) + \frac{D}{2}\log A(\varepsilon) = C + \frac{D}{2}\log A(\varepsilon) \quad ---(6)$$

Where C was a constant, and D_m=2*D/2 was the soil single fractal dimension [29].

3 Results and Discussion

3.1 Effects of Irrigation with Treated Wastewater and Saline-Sodic Solutions with Different SAR Levels on Soil K_s

Effect of different irrigation waters on soil K_s was shown in Fig.2. It can be observed that after simulated irrigation for 1 and 2 years later, soil K_s in the following descending order: simulated irrigation with CK > SAR3 > WW > SAR10 > SAR20, which meant the irrigation water types and SAR levels in waters determined the soil K_s, but the irrigation frequency did not affects the soil K_s, and the soil K_s decrease amplitude of simulated irrigation for 2 years was smaller than 1 year. Compared with initial value of the soil K_s, after simulated irrigation for 1 year, the K_s of all treatments decreased significantly, because irrigation water caused the certain scour to surface soil and changed the soil structure. In the circumstance of irrigation water with the approximately equal SAR level, the soil K_s irrigation with treated wastewater was smaller than saline–sodic solutions, it might be the reason that the soil pores block caused by suspended solid particles, and the dispersion of soil caused by dissolved organic matter had a greater effect on soil structure than the dispersion of soil clay

and aggregate caused by sodium in treated wastewater. The soil K_s irrigation with saline–sodic solutions had the descending order: simulated irrigation with SAR3 > SAR10 > SAR20, and the higher level of SAR in irrigation solutions, the smaller of the soil K_s, and similar effects on soil hydraulic conductivity had been reported [8].

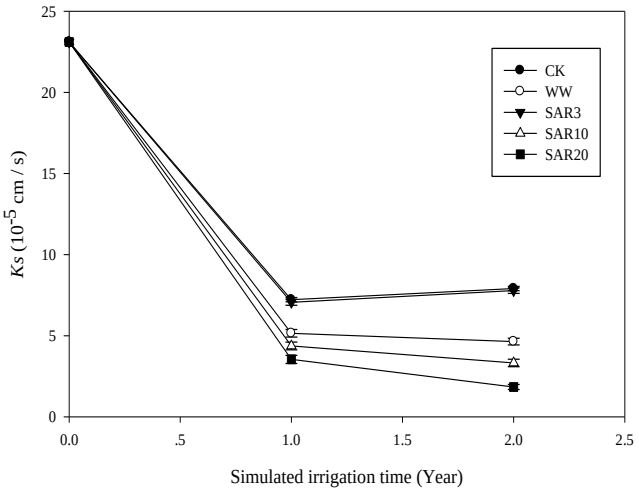

Fig. 2. Effects of irrigation waters on soil K_s

3.2 Effects of Irrigation with Treated Wastewater and Salin–Sodic Solutions with Different SAR Levels on Soil Pores Distribution

Soil binary images after simulated irrigation for 1 and 2 years was shown in Fig.3. In the soil binary images, the soil pores was black and solid was white. CS was the soil initial binary image, it had the largest area of single soil pore and decreased gradually from outside to inside, but its pores quantity were increasing. CK-1 and CK-2 binary images had the similar soil pores distribution, and except for a few macro-pores, many pores had a small area, and the macro-pores unevenly distributed in the small pores. WW-1 and WW-2 binary images also had the similar soil pores distribution, most of the pores had the same area, but compared with WW-2, WW-1 binary image had a smaller average pores area. SAR3-1 and SAR3-2 binary images had a great difference in soil pores distribution, after simulated irrigation for 1 year, the soil pores distribution looked like continuous rolling mountains, but after simulated irrigation for 2 years, the single pore area of a few soil pores became larger. SAR10-1 and SAR10-2 binary images also had a great difference in soil pores distribution, compared with simulated irrigation for 1 year, all soil macro-pores disappeared after simulated irrigation for 2 years. As for SAR20-1 and SAR20-2 binary images, compared with simulated irrigation for 1 year, soil macro-pores quantity increased almost 2 times, and the distribution of soil pores was relatively more uniform. Different irrigation soils had different pores distribution characteristics, which was similar with the findings of Li et al [30]. In conclusion, CS binary image had the

largest area of single soil pore but the smallest pores quantity, after simulated irrigation for 1 and 2 years, all soil binary images had a smaller single soil pore area but larger pores quantity. The distribution of pores irrigation with ordinary water and treated wastewater had the similar pores distribution after simulated irrigation for 1 and 2 years, respectively. In soil binary images irrigation with saline-sodic solutions, simulated irrigation frequency affected the distribution of pores, and at the different SAR levels, the change trend with irrigation frequency were also difference.

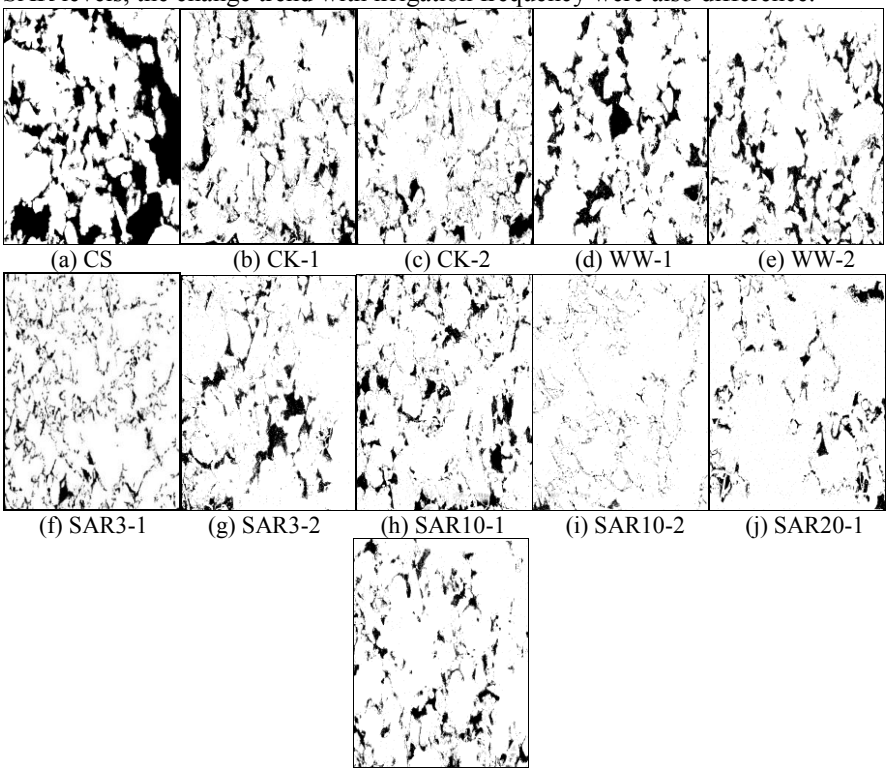

Fig. 3. The soil binary images (CS denoted initial binary image, -1 and -2 denoted soil binary image that simulated irrigation for 1 and 2 years, respectively, similarly hereinafter)

3.3 Effects of Irrigation with Treated Wastewater and Saline–Sodic Solutions with Different SAR Levels on Soil Pores Single Fractal Dimension

According to the formula (6), soil pores single fractal dimension (D_m) was twice as large as the slope of the double-log curve between $L(\varepsilon)$ and $A(\varepsilon)$. Soil D_m changed with different irrigation water was shown in Fig.4. The slope of the fitting line (half of the D_m) in Fig.4-CS was the smallest, the slope of the fitting lines were increased after simulated irrigation. Except for CK treatment, all other treatments had a larger slope after simulated irrigation for 2 years than 1 year. Except for the fitting line of the CS and SAR10-2 had a R^2 with 0.891 and 0.835, respectively, all other treatments had a $R^2 \geq 0.900$, which meant $LogA(\varepsilon)$ and $LogL(\varepsilon)$ showed a good linear correlation

relationship, and soil surface pores structure had a good self-similarity, namely fractal features. WW-1 and WW-2 had the biggest R^2 values, and simulated irrigation with treated wastewater had the best fitting effect.

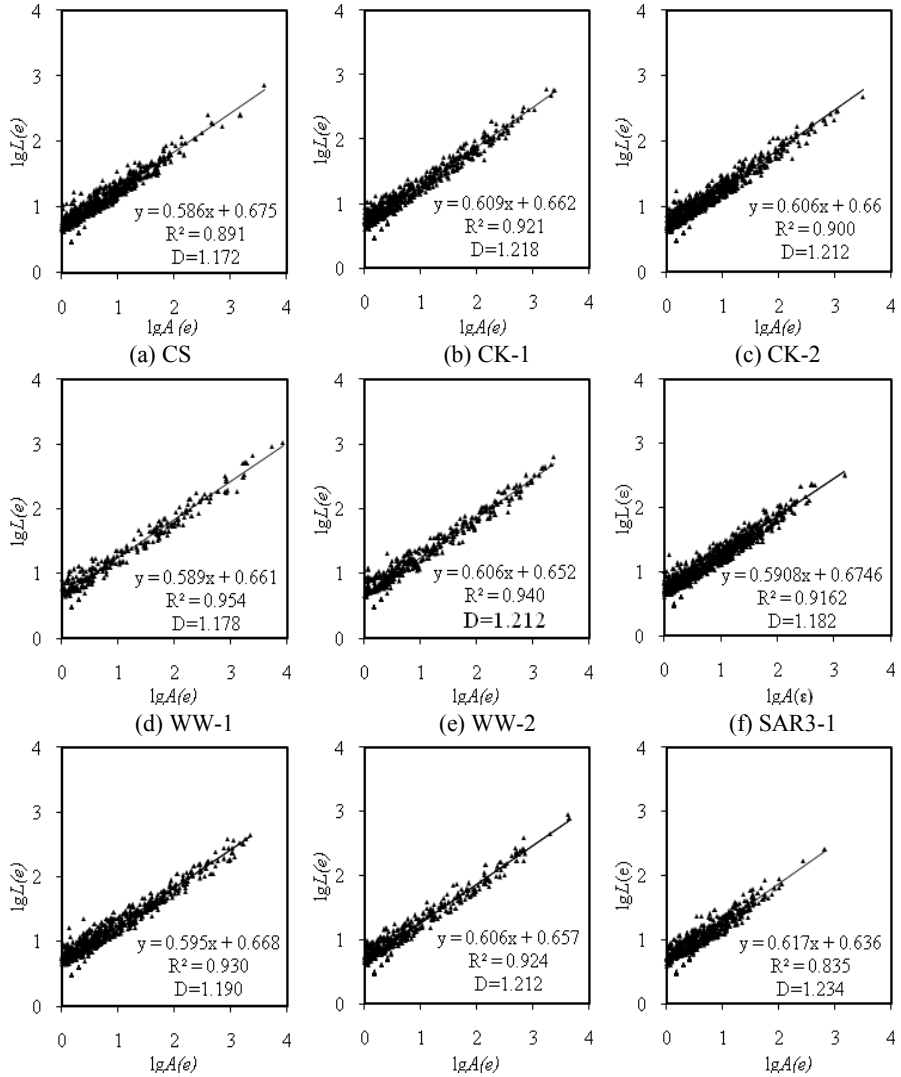

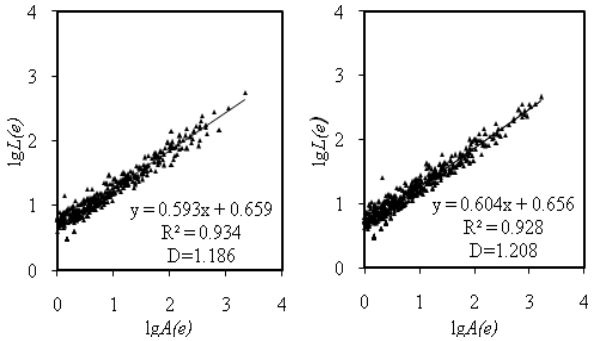

(j) SAR20-1 (k) SAR20-2

Fig. 4. Soil pores single fractal dimension (D_m) that based on digital image

Soil D_m with different irrigation water and simulated irrigation time was shown in Fig.5. Irrigation water changed the soil structure, and the soil D_m increased after simulated irrigation, which meant soil pores distribution became more complex. Except for CK treatment, soil D_m increased with the longer of simulated irrigation times. Soil D_m became the largest after simulated irrigation with ordinary water for 1 year, and irrigation with ordinary water caused the most serious erosion on surface soil. Soil D_m became the smallest after simulated irrigation with treated wastewater for 1 year, it might because the plugging and filling of suspended particles and dissolved organic matter in treated wastewater made the soil pore well –distributed. Among soils irrigation with saline–sodic solutions, SAR level of 10 had the largest soil D_m after simulated irrigation for 2 years, soil D_m did not increase with increasing SAR in irrigation waters. The accuracy of the soil D_m that obtained through the digital image analysis method depended on the discretion of resolution of grey scale image came from original soil thin section. In order to get more accuracy soil D_m, it was necessary to improve the discretion of resolution of soil thin section.

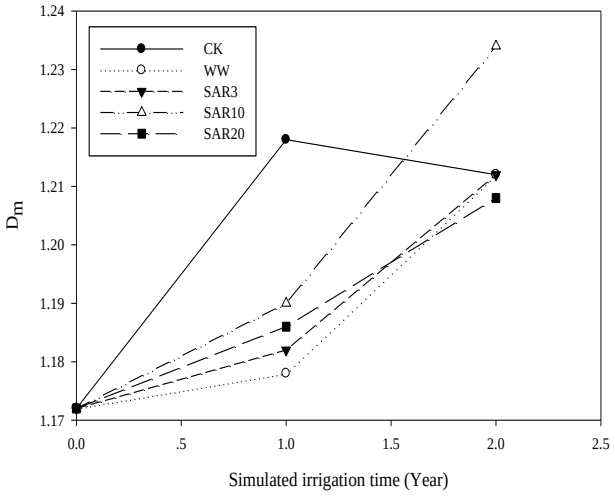

Fig. 5. Soil pores single fractal dimension (D_m) after simulated irrigation with different waters

3.4 The Correlation Relationship Between Soil K_s, D_m, and Relative Values of SAR Irrigation to Soils

The correlation relationship between soil K_s, D_m and relative values of SAR irrigation to soils were shown in Fig.6. The initial soil K_s and D_m data were not included in the Fig.6. According to SAR levels in irrigation water and the time of simulated irrigation, the relative values of SAR irrigation to soils were set, and CK-1, CK-2, WW-1, WW-2, SAR3-1, SAR3-2, SAR10-1, SAR10-2, SAR20-1 and SAR20-2 was 0.74, 1.48, 2.75, 5.5, 3, 6, 10, 20, 20 and 40, respectively. The linear correlation relationship between soil K_s and the relative values of SAR was: y (K_s) = -0.143 x (SAR) + 6.855, and R^2 = 0.714 (Fig.6-A), which meant they had a good linear correlation relationship, and with the increase of SAR levels in irrigation waters and the longer of simulated irrigation times, the soil K_s linear decreased. The linear correlation relationship between soil D_m and the relative values of SAR was: y (D_m) = 0.000 x (SAR) + 1.200, and R^2 = 0.025 (Fig.6-B), which meant they had a very weak linear correlation relationship, and the relationship among soil D_m, the SAR levels of irrigation water and irrigation frequency were very complicated, the electrolyte concentration in saline-sodic water and special material in treated wastewater might all affect the soil D_m. The linear correlation relationship between soil D_m and the soil K_s was: y (D_m) =0.001x (K_s)^2-0.02 x (K_s) + 1.247, R^2 = 0.142 (Fig.6-C), which meant they had a weak parabola correlation relationship. When used soil D_m represented soil pores structure of soil binary image based on the electron microscope scanning, it couldn't better reflect the relationship with soil K_s, because surface soil pores structure just reflected the distribution characteristics of soil pores on horizontal direction, and couldn't reflect the soil pores on the vertical direction.

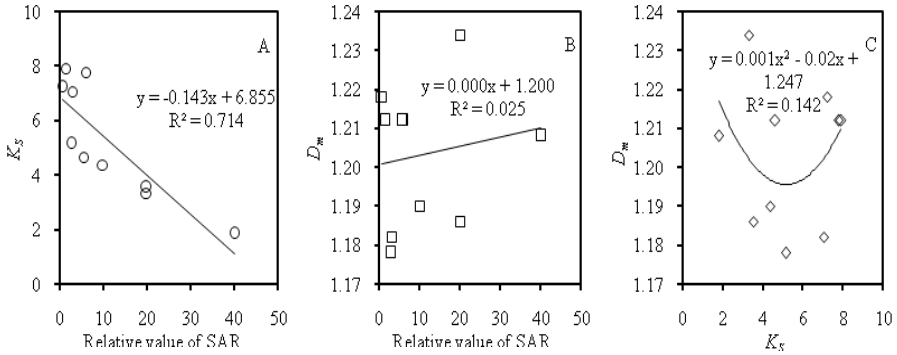

Fig. 6. The correlation relationship between soil K_s, D_m, and relative values of SAR in irrigation to soils (A: the correlation between the relative value of SAR and soil K_s; B: the correlation between the relative value of SAR and soil D_m; C: the correlation between soil *Ks* and D_m)

4 Conclusions

After simulated irrigation to soils in soil bins with ordinary water, treated wastewater and saline-sodic solutions with different SAR levels for 1 and 2 years, the results showed that soil K_s in the following descending order: simulated irrigation with CK > SAR3 > WW > SAR10 > SAR20, and the soil pores plugging caused by suspended solid particles, and the dispersion of soil caused by dissolved organic matter had a greater effect on soil structure than the dispersion of soil clay and aggregate caused by sodium in treated wastewater. After simulated irrigation, soils had a smaller single soil pore area but larger pores quantity, and the distribution of soil pores which was irrigated with treated wastewater had the similar pores distribution after simulated irrigation for 1 and 2 years, but for treatments irrigated by saline-sodic solutions, simulated irrigation frequency affected the distribution of pores, and with the difference of SAR levels, the change trend with time were also difference. The results also showed the soil pores structure binary image was an effective method to analysis soil pores. Soil D_m increased after simulated irrigation, and the smallest was the soil simulated irrigation with treated wastewater for 1 year, because the plugging and filling of suspended particles and dissolved organic matter in treated wastewater made the soil pore well-distributed, and the soil D_m did not increased with increasing of SAR in irrigation waters. Irrigation with treated wastewater had a greater effect on soil K_s than soil D_m, comparing with saline-sodic solutions which had the similar SAR. The relative values of SAR irrigation to soils and soil K_s had a good linear correlation relationship, while the soil D_m and the relative values of SAR irrigation to soils had a very weak linear correlation relationship. The soil D_m calculated from soil binary images could not well reflect the soil K_s, thus future research should consider both the horizontal and vertical directions of soil D_m to reflect the hydraulic conductivity of saturated soil.

Acknowledgment

Funds for this research was provided by the Public Welfare Project of Ministry of Water Resources of China (No.201101051), and the National Natural Science Foundation of China (No.51279204).

References

1. Yi Lili, Jiao Wentao, Chen Xiaoning et al. An Overview of Reclaimed Water Reuse in China[J]. Journal of Environmental Sciences, 2011, 23(10): 1585-1593.
2. Minhas P. S., Sharma D. R. Hydraulic Conductivity and Clay Dispersion as Affected by the Application Sequence of Saline and Simulated Rain Water[J]. Irrigation Science, 1986, 7(3): 158-167.
3. Minhas P. S., Singh Y. P., Chhabba D. S. et al. Changes in Hydraulic Conductivity of Soils Varying in Calcite Content under Cycles of Irrigation with Saline-Sodic and Simulated Rain Water[J]. Irrigation Science, 1999, 18(4): 199-203.

4. Sun Jiaxia, Kang Yaohu, Wan Shuqin et al. Soil Salinity Management with Drip Irrigation and its Effects on Soil Hydraulic Properties in North China Coastal Saline Soils[J]. Agricultural Water Management, 2012, 115(4):10-19.
5. Zhang Guosheng, Chan K. Y., Li G. D. et al. The Effects of Stubble Retention and Tillage Practices on Surface Soil Structure and Hydraulic Conductivity of a Loess Soil[J]. Acta Ecologica Sinica, 2011, 31(6): 298-302.
6. Gharaibeh M. A., Eltaif N. I., Al-Abdullah B. Impact of Field Application of Treated Wastewater on Hydraulic Properties of Vertisols[J]. Water, Air, and Soil Pollution, 2007, 184(1-4): 347-353.
7. Viviani G., Iovino M. Wastewater Reuse Effects on Soil Hydraulic Conductivity[J]. Journal of Irrigation and Drainage Engineering, 2004, 130(6): 476-484.
8. Frenkel H., Goertzen J. O., Rhoades J. D. Effects of Clay Type and Content, Exchangeable Sodium Percentage, and Electrolyte Concentration on Clay Dispersion and Soil Hydraulic Conductivity[J]. Soil Science Society of America Journal, 1978, 42(1): 32-39.
9. Felhendler R., Shainberg I., Frenkel H. Dispersion and Hydraulic Conductivity of Soils in Mixed Solutions[C]. Proceedings of the Transition of the 10th International Congress of Soil Science, Moscow, Nauka Pub. House, 1974, 103-112.
10. Lado M., Ben-Hur M. Effects of Irrigation with Different Effluents on Saturated Hydraulic Conductivity of Arid and Semiarid Soils[J]. Soil Science Society of America Journal, 2010, 74(1): 23-32.
11. Mahdy A. M. Soil Properties and Wheat Growth and Nutrients as Affected by Compost Amendment under Saline Water Irrigation[J]. Pedosphere, 2011, 21(6): 773-781.
12. Singh R. B., Minhas P. S., Chauhan C. P. S. et al. Effect of High Salinity and SAR Waters on Salinization, Sodication and Yields of Pearl-Millet and Wheat[J]. Agricultural Water Management, 1992, 21(1-2): 93-105.
13. Mandelbort B. B. The Fractal Geometry of Nature[M]. New York: W. H. Freeman and Company, 1983, 1-8.
14. Tyler S. W., Wheatcraft S. W. Application of Fractal Mathematics to Soil Water Retention Estimation[J]. Soil Science Society of America Journal, 1989, 53(4): 987-996.
15. Perrier E., Bird N., Rieu M. Generalizing the Fractal Model of Soil Structure: The Pore-Solid Fractal Approach[J]. Geoderma, 1999, 88(3-4): 137-164.
16. Caruso T., Barto E. K., Siddiky M. R. K., et al. Are Power Laws that Estimate Fractal Dimension a Good Descriptor of Soil Structure and Its Link to Soil Biological Properties?[J] Soil Biology and Biochemistry, 2011, 43(2): 359-366.
17. Crawford J. W., Pachepsky Y. A., Rawls W. J. Integrating Processes in Soils Using Fractal Models[J]. Geoderma, 1999, 88(3-4): 103-107.
18. Dathe A., Eins S., Niemeyer J., et al. The Surface Fractal Dimension of the Soil-Pore Interface as Measured by Image Analysis[J]. Geoderma, 2001, 103(1-2): 203-229.
19. Zhao Shiwei, Su Jing, Yang Yonghui et al. A Fractal Method of Estimating Soil Structure Changes under Different Vegetations on Ziwuling Mountains of the Loess Plateau, China[J]. Agricultural Sciences in China, 2006, 5(7): 530-538.
20. Guan Xiaoyan, Yang Peiling, Ren Shumei, et al. Multifractal Analysis of Soil Structure under Long-Term Wastewater Irrigation Based on Digital Image Technology[J]. New Zealand Journal of Agricultural Research, 2007, 50(5): 789-796.
21. Vogel H. J., Kretzschmar A. Topological Characterization of Pore Space in Soil—Sample Preparation and Digital Image-Processing[J]. Geoderma, 1996, 73(1-2): 23-38.
22. Ahmadi A., Neyshabouri M. R., Rouhipour H., et al. Fractal Dimension of Soil Aggregates as an Index of Soil Erodibility[J]. Journal of Hydrology, 2011, 400(3-4): 305-311.
23. Bird N., Díaz M. C., Saa A., et al. Fractal and Multifractal Analysis of Pore-Scale Images of Soil[J]. Journal of Hydrology, 2006, 322(1-4): 211-219.

24. Dathe A., Tarquis A. M., Perrier E. Multifractal Analysis of the Pore-and Solid-Phases in Binary Two-Dimensional Images of Natural Porous Structures[J]. Geoderma, 2006, 134(3-4): 318-326.
25. Li Yi., Li Min., Horton R. Single and Joint Multifractal Analysis of Soil Particle Size Distributions[J]. Pedosphere, 2011, 21(1): 75-83.
26. Murphy C. P. Thin Section Preparation of Soils and Sediments[M]. UK: A. B. Academic Publishers, 1986, 20-30.
27. Guan Xiaoyan. The Quantitative Simulation of Soil Quality at Different Scales under the Reclaimed Water Irrigation[D]. Beijing: China Agricultural University, 2009, 42-45.
28. Mandelbrot B. B., Passoja D. E., Paullay A. J. Fractal Character of Fracture Surfaces of Metals[J]. Nature, 1984, 308(5961): 721-722.
29. Li Yunkai, Xu Tingwu, OuYang Zhiyun et al. Micromorphology of Macromolecular Superabsorbent Polymer and its Fractal Characteristics[J]. Journal of Applied Polymer Science, 2009, 113(6): 3510-3519.
30. Li Decheng, Velde B., Zhang Taolin. Study on Soil Pore Characteristics on Small Scale by Using Techniques of Serial Digital Images[J]. Acta Pedologica Sinica, 2003, 40(5): 521-528.